ELSEVIER

Quartz-crystal microbalance for *in situ* monitoring of laser cleaning of carbon nanotubes ☆

Katherine E. Hurst [a], Abram Van Der Geest [a,b], Mark Lusk [b], Elisabeth Mansfield [a], John H. Lehman [a,*]

[a] *National Institute of Standards and Technology, Boulder, CO 80305, USA*
[b] *Colorado School Mines, Golden, CO, USA*

ARTICLE INFO

ABSTRACT

Photochemical changes of single-walled carbon nanotubes, graphite and amorphous carbon have been investigated with a quartz-crystal microbalance (QCM). The method of *in situ* measurements reduces our uncertainty that is attributable to environmental variables, such as relative humidity and temperature. At 248 nm, near the resonance of the π-plasmon we expect the interaction of laser light and carbon nanotube material to exhibit relatively high absorptivity. We discuss the importance of the single-walled carbon nanotube surface plasmon in the reduction of carbon impurities. The QCM is a means to quantify laser damage with respect to irradiance, pulse width and exposure time.

1. Introduction

Single-walled carbon nanotube (SWCNT) material has unique thermal, electrical, and chemical properties for use in a broad range of applications. However, impurities are often also formed during the nanotube synthesis process, and then additional purification is required. Previously, we demonstrated selective oxidation of carbon impurities in as-prepared SWCNT samples by exposure to 248 nm laser light [1,2]. We reported modifications of the SWCNT material with respect to exposure duration, atmosphere and irradiance [1]. Evidence of laser-induced damage and photochemical changes of the SWCNT material obtained from these studies has shown a unique interaction between 248 nm laser light (5 eV) and a plasmon resonance at 5 eV. In the past, our measurement tools, such as imaging and Raman spectroscopy, have been largely qualitative. In the present work, we emphasize the novel use of a quartz-crystal microbalance (QCM) as a quantitative *in situ* method to measure laser-induced purification of carbon nanotubes.

The QCM technique exploits the piezoelectric properties of a quartz crystal that vibrates when an oscillating electric field is applied to electrodes on each face. The geometry, orientation and speed of sound of the quartz along with the mass of any film in contact at the surface define a resonance condition. The series resistance of the quartz resonator will change when the vibrating energy is dissipated in the contacting film. For an evenly deposited layer, the resonant frequency of the crystal will decrease proportionally to the mass of the film.

The QCM has been used previously to investigate the deposition, functionalization, adsorption, and other reactivity of carbon nanotubes by measuring mass changes as small as 1×10^{-9} g [3–5]. *In situ* QCM measurements have also been used to characterize solution-phase layer-by-layer assembly of multi-walled CNT-based [4,6] and SWCNT complexes [5,6]. Recently, Mansfield et al. reported very good agreement between QCM and thermogravimetric analysis (TGA) techniques for the oxidation of carbon nanotubes [7]. A specific correction was considered that addresses adsorbed atmospheric water vapor on the nanotube sample. Also, both Su

et al. and Zhang et al. have demonstrated that accurate and repeatable mass measurements on carbon nanotubes are difficult because nanotubes are sensitive to environmental changes such as the relative humidity [3,5]. Hence, in this work, we employ QCM measurements *in situ* to minimize local environmental effects (such as laboratory temperature, humidity, or air currents), as well as spatial variation of electrical contact between the crystal and electrodes. Additionally, real-time characterization reduces temporal effects, such as atmospheric gas adsorption.

2. Experimental

Amorphous carbon, graphite, nickel particles (each from Sigma–Aldrich) [8] and commercially available arc-discharge generated SWCNT samples were examined. Each sample was sonicated in chloroform using a probe tip sonicator for 3 min, followed by an ultra-sonication bath for 30 min. Each sample was then deposited on its own 5 mm diameter AT-cut quartz-crystal having gold patterned electrodes on each face. The crystal was masked prior to coating in order to define an area overlapping the electrode, but not covering the entire face of the crystal. The carbon material was applied using an airbrush such that only a thin film of approximately 2–8 μg of sample was deposited onto the surface of the electrode. The frequency of the crystal was monitored using a Stanford Research Systems QCM200a [8] that applied an oscillating electric field across the crystal to induce shear-mode vibrations at a resonant frequency of 5 MHz. The motional inductance increases when mass is added to the crystal electrode, which changes the resonant frequency. The frequency shift of the resonance is proportional to the added mass. A schematic of the experimental set-up is shown in Fig. 1.

A krypton fluoride (KrF) excimer laser operating at 248 nm, 20 ns pulse duration and a 10 Hz repetition rate was used to irradiate the samples. The beam was spatially homogenized, resulting in a square area of $1 \times 1 \text{ cm}^2$, which was greater than the 0.4 cm^2 active area of the QCM electrode. The irradiance for each exposure was kept constant at approximately 300 mW/cm^2. This irradiance was chosen based upon our previous work, in which exposure for a 30 s period indicated a reduction on carbon impurities without the creation of new defects in the nanotubes [1]. The resonance frequency of the crystal was monitored continuously as the sample was exposed to the laser. Exposure periods were 15 s followed by approximately 4 min between exposures in order to obtain

an accurate measurement of the resonance frequency at equilibrium.

The mass of the material on the crystal was calculated based on the Sauerbrey equation, shown in Eq. (1). Here, the change in mass, Δm, is directly proportional to the change in resonant frequency of the crystal, Δf.

$$\Delta m = \frac{-A\sqrt{\rho\mu}}{2f_0^2}\Delta f \qquad (1)$$

Also, f_0 is the resonant frequency of a bare quartz crystal, A is the active area of the electrode and ρ and μ are the density shear modulus of quartz. An important attribute of employing the relation in Eq. (1) is that the mass of the film can be determined independently of the material properties and based solely upon the well-known properties of quartz. This relationship is true for thin films, where the deposition of material results in a shift in frequency of less than 2% [9].

It is necessary to establish some basis for the uncertainty of Δm. The values of ρ and μ for quartz do not measurably change near room temperature following the laser exposure (the 4 min while the laser is off between exposure periods). Thus, the uncertainty of Δm depends primarily on Δf. We consider the change in Δf with no load on the QCM (no mass loss) as a basis of the uncertainty and the relative mass changes. The uncertainty for the data in Fig. 2 is based on the measured change in resonant frequency Δf for an uncoated crystal after five exposure periods of 15 s. Spikes in the resonant frequency, attributed to crystal heating occurring during the exposure period, were observed similarly to those shown in Fig. 2, however the maximum difference in Δf between exposure periods was used to calculate an uncertainty of 1.5 ng.

3. Results

Fig. 2 shows the change in resonant frequency response and the corresponding mass of the SWCNT film measured during the laser exposure. During each 15 s laser exposure, the resonant frequency increased and asymptotically stabilized at a new resonance corresponding to the reduced mass. The large spikes in the resonance frequency, evident in Fig. 2, mark the 15 s irradiation of the sample by the laser. These spikes are
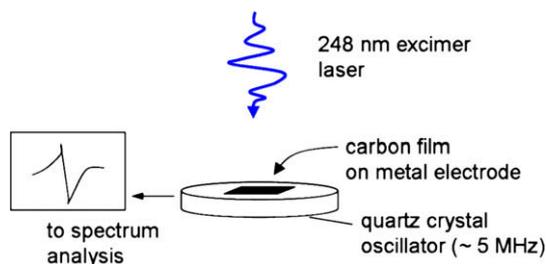

Fig. 1 – A schematic of the experimental set-up in which the 248 nm laser light interacts with the carbon film while the oscillation of the QCM crystal is recorded.
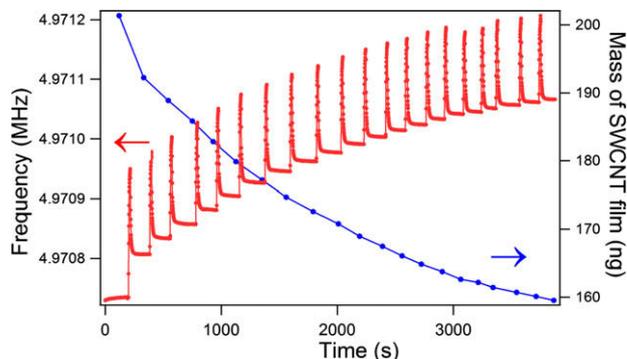

Fig. 2 – The frequency and mass of a QCM crystal coated with SWCNT film and the associated mass changes upon exposure to laser irradiation at 248 nm. The uncertainty of the mass measurement is 1.5 ng for the duration of the measurement.

consistent with the rapid and temporary temperature change of the bulk crystal during exposure to the laser light. The mass change calculated with Eq. (1) is plotted versus the right axis in Fig. 2.

The calculated mass change for three different carbon samples: amorphous carbon, graphite and SWCNT films are shown in Fig. 3. For comparison, all mass changes are shown as percent weight change. The calculated mass change for the each sample is based on the initial carbon content. The amount of metallic impurities in both the amorphous and graphite samples was negligible; however, the as-prepared SWCNT films had residual metal catalysts accounting for approximately 35% of the sample mass [10]. Therefore, the mass of the sample at each data point in Fig. 3 is adjusted to account for the metallic content in the original sample. The greatest mass loss was observed for the SWCNT sample. The sample mass was reduced by 32% after exposure to 300 s of cumulative exposure time. Amorphous carbon and graphite exhibited 2.6% and 15.2% changes in mass, respectively, after 120 s of cumulative exposure time. After the first 15 s exposure of graphite, 12.6% of mass was lost; however, the sample then lost only an additional 2.8% of mass for longer exposure periods.

Scanning electron microscopy (SEM) images before and after 300 s cumulative laser exposure are shown in Fig. 4a and b. These images show greater definition of bundles for the treated sample compared to the untreated sample consistent with the removal of the carbon coating. The catalyst particles also appear to have greater definition. In our earlier work we showed transmission electron microscope (TEM) images of a single MWCNT before and after exposure to 248 nm irradiation. These images indicate the surrounding carbon coating was exfoliated from the nanotube surface after treatment [11].

Raman spectroscopy at 488 nm was also used to characterize the purity and verify the presence of single-walled nanotubes. Radial breathing modes of the nanotubes at 170 cm^{-1} were evident before and after 300 s cumulative laser exposure, demonstrating that the nanotubes survived the laser treatment. This is consistent with our previous findings wherein the diameter distribution did not change after exposure to the laser irradiation [1].

Fig. 4 – SEM images of a SWCNT film (a) before, and (b) after laser irradiation for 300 s cumulative exposure.

4. Discussion

As previously suggested [1,2], we propose that the π-plasmon resonance centered at 5 eV (∼248 nm) overlapping the 248 nm light is responsible for the removal of carbon impurities. This interaction of light and matter creates an enhanced electromagnetic (EM) field surrounding the nanotube, which increases the concentration of excited bonds and enhances the rate of oxidation. Absorption by the plasmon resonance and the associated thermalization may simply heat the surrounding carbon impurities to a point at which the rate of oxidation is enhanced. Thus, the favorable thermal properties of nanotubes compared to amorphous carbon impurities provide a means of selective oxidation [2]. Additionally, the locally enhanced EM field also increases the concentration of activated bonds surrounding the amorphous carbon impurities [12]. Oxidation may then proceed more rapidly, because the rate is proportional to this concentration.

It is difficult to distinguish the mass of the carbon impurities (as opposed to the mass of the carbon nanotubes) in the as-prepared sample in order to determine the overall efficiency of the purification. However, the mass change associated with exposure period to 248 nm light of the as-prepared nanotube sample is significantly different from either of the representative carbon nanotube impurities. Aside from the large initial mass loss for graphite, neither the graphite nor the amorphous carbon samples exhibited a
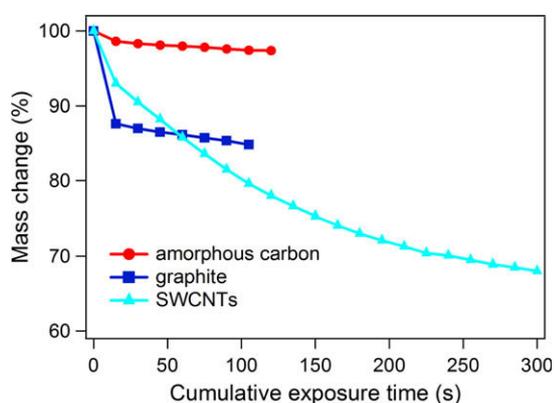

Fig. 3 – The calculated mass change based upon QCM measurement for amorphous carbon, SWCNT film and graphite exposed to 15 s periods of 248 nm laser irradiation.
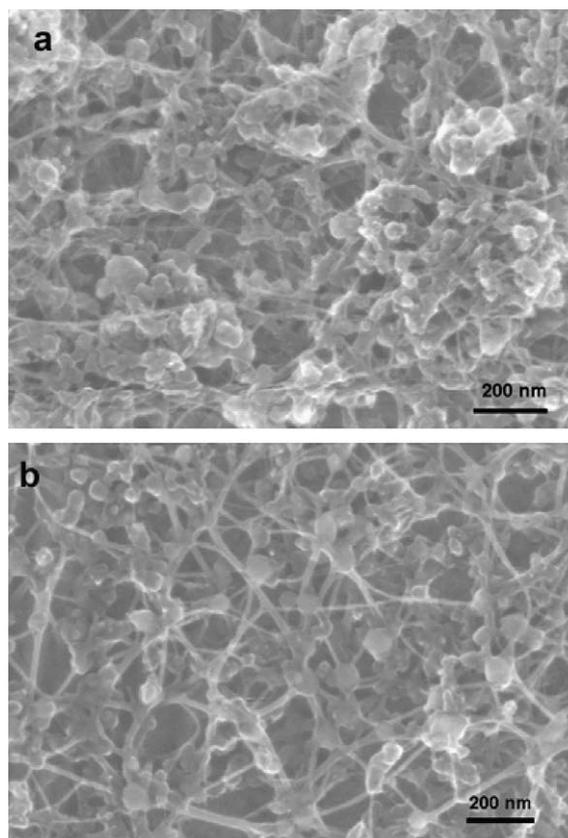
Table 1 – Analysis of Raman spectroscopy before and after 300 s cumulative laser exposure.

	D/G intensity ratio	FWHM of the D-band (cm^{-1})
As prepared	0.039	39.7
300 s cumulative exposure	0.021	15.25

large rate of mass loss with longer exposure periods, while the rate of mass loss for the nanotube sample gradually decreased and leveled off after 250 s of exposure. For each sample shown in Fig. 2, the greatest change in mass occurs after the first 15 s exposure. This initial mass loss is likely representative of the desorption of water and other adsorbed atmospheric gases on the carbon film surface. As previously noted, carbon samples have a high affinity for water vapor [3,5,7]. It is also possible that the most reactive carbon impurities are oxidized during this first exposure, with the buried carbon impurities being exposed more slowly. Dumont et al. investigated 248 nm laser interaction on a pulse-by-pulse basis, with particular attention to the first single pulse [13]. It is possible that the initial mass loss follows the first pulse rather than the cumulative first exposure.

Raman spectroscopy revealed a significant increase in the purity of the nanotube sample after exposure to 300 cumulative seconds to the laser light. Analysis of the D-band at 1350 cm^{-1}, which arises due to symmetry-lowering effects, and the G-band at 1590 cm^{-1}, which is attributed to the in-plane vibrations of a graphitic plane, are commonly used to characterize the relative purity of the SWCNT sample [14]. The ratio of the intensity of the D-band to that of the G-band provides a measure of the number of defects in the nanotube sample. After exposure to 300 cumulative seconds of laser light, the D/G ratio decreased from 0.039 (for as-prepared material) to 0.021, as listed in Table 1. The full-width-at-half-maximum (FWHM) of the D-band characterizes the relative amount of carbon impurities in the sample. The narrowing of the D-band FWHM from 39.7 cm^{-1} (for as-prepared) to 15.25 cm^{-1} for the sample after laser irradiation demonstrates the removal of non-nanotube carbons from the sample. Such a low FWHM is consistent with highly purified SWCNT material [14]. In contrast, the D-band FWHM for amorphous carbon remained constant (42–45 cm^{-1}) with increased UV laser exposure time. Future work will benefit from the analysis of D′ and G′ for carbon materials exposed to 248 nm irradiation.

It has been well documented that residual catalyst metal impurities can affect the oxidation of the carbon material in the sample [15]. The exothermic reaction of metallic oxidation can create localized heating and cause pre-ignition of surrounding carbon material. Therefore, an additional experiment was performed to affirm that the effect of the metal particles was negligible. A sample of 25% by weight of nickel particles was mixed with graphite and exposed to 15 s exposures until there was no change in the resonance of the crystal with further exposure. The mass loss based upon the original carbon amount was only 3.6% by mass, which is less than that observed for the graphite sample without metal particles. Therefore, if a heating mechanism attributable to the metal particles was important in the laser interaction, a

greater loss of mass would have been expected in the graphite sample with the metal particles. Thus, the catalyst metals in the as-prepared nanotube samples do not enhance the amount of carbon oxidized when exposed to 248 nm light. It is possible that there was an increase in mass due to the oxidation of metal particles, and this increase in mass could be superimposed on the loss of mass the carbon sample. Oxidation of metallic particles in the as-prepared nanotube material is not enhanced by the surface plasmon interaction, because the frequency of the enhanced field is outside the resonance of the metallic particles. Therefore, we expect the likelihood of metal oxidation to be similar for metal particles in the as-prepared SWCNT sample to that for the metal particles mixed with graphite.

The π-plasmon of sp^2-bonded carbon in graphite is also resonant with the 248 nm photons. We have considered whether excitation of the π-plasmon from sp^2 carbon in graphite might facilitate the oxidation of amorphous carbon by exposing a sample consisting of 50% amorphous carbon and 50% graphite. The resonance frequency remained nearly constant after 30 s cumulative exposure, and the increase in resonant frequency was proportional to a loss of mass of only 4.7% after 75 s. This relatively low loss of mass suggests that it is not simply the photoexcitation of sp^2 carbon that aids the removal or oxidation of sp^3 carbon; it demonstrates the importance of excitation of the nanotube surface plasmon that results in the purification. This interaction has been investigated in greater detail by density-functional-theory modeling [12].

5.   Conclusion

We have demonstrated the use of QCM measurement *in situ* for mass changes associated with the photochemical oxidation of as-produced carbon nanotube samples. The results demonstrate that a distinct interaction between 248 nm laser light and SWCNTs exists that is not observed for amorphous carbon or graphite. *In situ* QCM provides a means to reduce the uncertainty of our measurements that would otherwise be attributable to environmental changes in the carbon samples such as relative humidity and temperature. The results are consistent with related work wherein the oxidation of carbon with 248 nm light is attributed to heating as well as electric field enhancement in proximity of the single-walled carbon nanotubes.

REFERENCES

[1] Hurst KE, Dillon AC, Keenan DA, Lehman JH. Cleaning of carbon nanotubes near the pi-plasmon resonance. Chem Phys Lett 2007;433(4–6):301–4.
[2] Hurst KE, Dillon AC, Yang S, Lehman JH. Purification of single wall carbon nanotubes as a function of UV wavelength,

atmosphere, and temperature. J Phys Chem C 2008;112(42):16296–300.

[3] Su PG, Tsai JF. Low-humidity sensing properties of carbon nanotubes measured by a quartz crystal microbalance. Sens Actuator B – Chem 2009;135(2):506–11.

[4] Xue W, Cui T. Characterization of layer-by-layer self-assembled carbon nanotube multilayer thin films. Nanotechnology 2007;18:145709–7.

[5] Zhang Y, Yu K, Xu R, Jiang D, Lou L, Zhu Z. Quartz crystal microbalance coated with carbon nanotube films used as humidity sensor. Sens Actuator a – Phys 2005;120:142–246.

[6] Sugikawa K, Numata M, Kaneko K, Sada K, Shinkai S. Alternate layer-by-layer adsorption of single- and double-walled carbon nanotubes wrapped by functionalized beta-1,3-glucan polysaccharides. Langmuir 2008;24(23):13270–5.

[7] Mansfield E, Kar A, Hooker SA. Application of quartz crystal microbalances at elevated temperatures as an alternative to TGA. Anal Chem, submitted for publication.

[8] Identification of commercial material does not imply recommendation or endorsement by the National Institute of Standards and Technology.

[9] Lu C-S, Lewis O. Investigation of film-thickness determination by oscillating quartz resonators with large mass load. J Appl Phys 1972;43(11):4385–90.

[10] Harutyunyan AR, Pradhan BK, Chang J, Cheng G, Eklund PC. Purification of single-wall carbon nanotubes by selective microwave heating of catalyst particles. J Phys Chem B 2002;106:8671–5.

[11] Singh G, Rice P, Hurst KE, Lehman JH, Mahajan RL. Laser-induced exfoliation of amorphous carbon layer on an individual multiwall carbon nanotube. Appl Phys Lett 2007;91:033101–4.

[12] Van der Geest AG, Hurst KE, Bronstein ND, Lehman JH, Lusk MT. Theoretical and experimental evidence of the role of electromagnetic resonance in the cleaning of nanotubes. Phys Rev B 2010;81(11):115440–8.

[13] Dumont T, Lazare S, Lippert T, Wokaun A. Changes in the etch rate of photosensitive polymers as a function of the pulse number. Appl Phys A – Mater Sci Process 2004;79(4–6):1271–4.

[14] Dillon AC, Yudasaka M, Dresselhaus MS. Employing Raman spectroscopy to qualitatively evaluate the purity of carbon single-wall nanotube materials. J Nanosci Nanotechnol 2004;4(7):691–703.

[15] Chiang IW, Brinson BE, Smalley RE, Margrave JL, Hauge RH. Purification and characterization of single-wall carbon nanotubes. J Phys Chem B 2001;105(6):1157–61.